Transactions, SMiRT-25
Charlotte, NC, USA, August 4-9, 2019
Division VII

PROBABILISTIC SSI ANALYSIS OF A REACTOR BUILDING TO FACILITATE FRAGILITY ASSESSMENT

Peter Rangelow[1], Tobias Richter[2], Vladimir Nincic[3], Andrii Nykyforchyn[4], Sunay Stäuble[5], and Manuel Pellissetti[6]

[1] Senior Expert, formerly Framatome GmbH, now Basler & Hofmann AG, Zürich, Switzerland
[2] Consultant, formerly Framatome Inc., now BHI Energy, San Jose, CA, USA
[3] Engineer, Framatome GmbH, Karlstein, Germany
[4] Director Earthquake Group, NPP Gösgen, Däniken, Switzerland
[5] Earthquake Engineer, NPP Gösgen, Däniken, Switzerland
[6] Senior Expert/Advisor, Framatome GmbH, Erlangen, Germany

INTRODUCTION

After the Fukushima Daiichi nuclear accident the Swiss Federal Nuclear Safety Inspectorate (ENSI) requested the nuclear power plants (NPP) in Switzerland to review their plant safety margin against the updated seismic hazard – denoted as ENSI-2015. Following ENSI requirements, the Gösgen NPP has to carry out probabilistic and deterministic accident analyses to evaluate the impact of the new seismic hazard on the plant safety margin and radiological risk.

For the evaluation of the seismic risk, structural analyses of the safety relevant buildings as well as development of Floor Response Spectra (FRS) for seismic analyses of equipment have been performed. For this purpose, a 3D finite-element model of the reactor building (RB), which is coupled with a 3D model of the primary and secondary circuit components and piping (Nuclear Steam Supply System; NSSS), has been developed.

In this paper the coupled 3D RB-NSSS model, the methodology utilized in probabilistic SSI analysis, preliminary probabilistic results (e.g. ISRS and their frequency dependent variabilities), insights gained from the probabilistic ISRS, and their applicability in fragility analysis are presented.

GROUND MOTION DEFINITION

The seismic hazard at the Swiss NPPs has recently been updated to more accurately reflect local seismicity. As a result, the ENSI-2015 seismic hazard assessment has been released for all Swiss NPP sites in 2016, see Stäuble et.al. (2018). The results are available in the form of Uniform Hazard Spectra (UHS) for annual frequencies of exceedance from 10^{-3}/a to 10^{-7}/a, at three elevations: site surface at ± 0.0 m, bottom of reactor building basemat at -9.0 m and limestone bedrock at -27.5 m. The median-centered UHS with an annual exceedance probability (AEP) of 10^{-4}/a is the basis for the probabilistic response evaluation, with a Peak Ground Acceleration (PGA) at the free field ground surface of 0.37 g and 0.21 g of the horizontal (see Fig. 1) and vertical components, respectively. The probabilistic SSI analysis is performed with 30 statistically independent sets of time histories (TH) evaluated as "within-layer" foundation input motions (FIM) at -9 m with a median PGA of 0.22 g and 0.14 g of the horizontal and vertical components, respectively, see Fig. 2. The procedure for deriving the ground motion THs ensures consistency with the seismic hazard background at the Gösgen site and compatibility with the requirements in US-NRC (2014). Each of the resulting 30 THs closely matches the target median UHS for 10^{-4}/a. However, the use of recorded time histories as seed motions introduces significant variability of other characteristic ground motion intensity measures, e.g. strong motion duration, Arias Intensity (AI), and Cumulative Absolute Velocity (CAV).

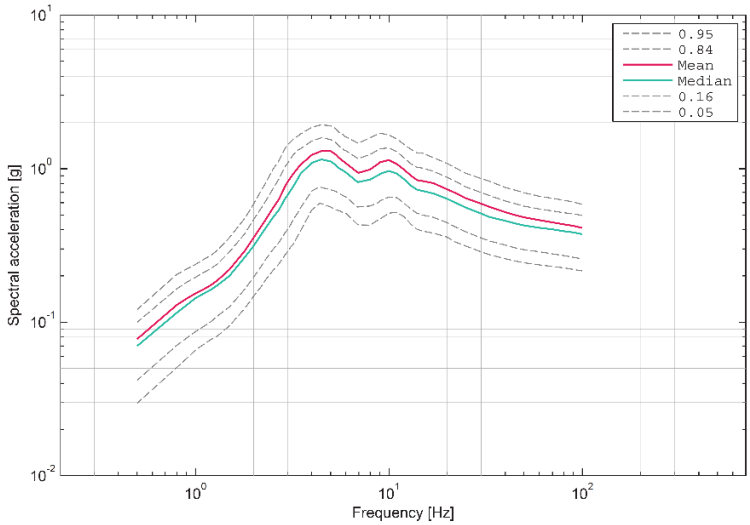

Figure 1. The ENSI-2015 UHS for an AEP of 10^{-4}/a at the ground surface, Horizontal, D = 5 %.

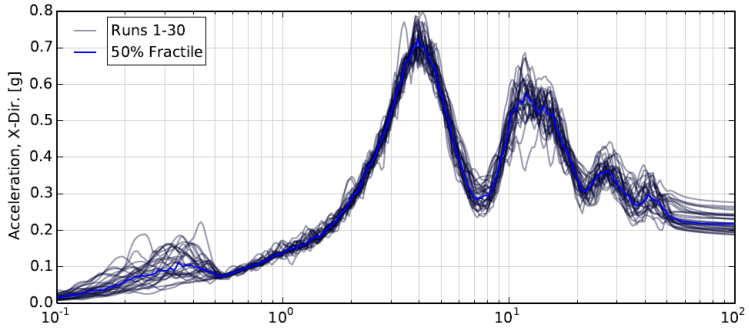

Figure 2. UHS-Compatible Foundation Input Motion Response Spectra (30 THs), Horizontal, D = 5 %.

SOIL MATERIAL PROPERTIES

The Gösgen NPP performed extensive site exploration/characterization in order to obtain detailed information on local soil properties, both for the assessment of ground motions and seismic geological effects like gravitational soil mass movements and soil liquefaction risks. The Quaternary section (sedimentary soil layer) consists of around 27.5 m well-graded, highly compacted gravel, which serves as competent medium for the plant. The corresponding shear wave velocity below grade is approx. 260 m/s, linearly increasing to approx. 730 m/s at 27.5 m depth. An underlying limestone formation characterizes the site with a shear wave velocity of 2500 m/s. An initial soil profile is developed as the mean of five profiles. The initial soil profile is iterated using SHAKE for 2×30 horizontal motions using appropriate degradation curves for shear modulus and soil damping. A final best estimate soil profile is obtained from the 60 individual soil profiles, which is interpreted as median centered. In the vertical direction a typical state-of-practice approach using the compression wave velocity is applied. In the next step the median soil profile is randomized in order to capture the variation of the soil at the site. The Latin Hypercube Sampling (LHS) technique is utilized to generate 30 scale factors to be applied to the shear modulus and soil damping. Thereby, a Coefficient of Variation (CoV) of 0.44 (target 0.45) is used for the shear modulus and 0.35 (target 0.35) for the soil damping. These assumptions yield scaling factors within the range of values between 0.41 and 2.59 for the shear modulus and 0.50 and 2.01 for the soil damping. Soil shear modulus and damping are correlated by a negative coefficient of -0.61. The LHS scale factors are used to generate 30 soil profiles for the soil-structure interaction analysis, see Fig. 3.

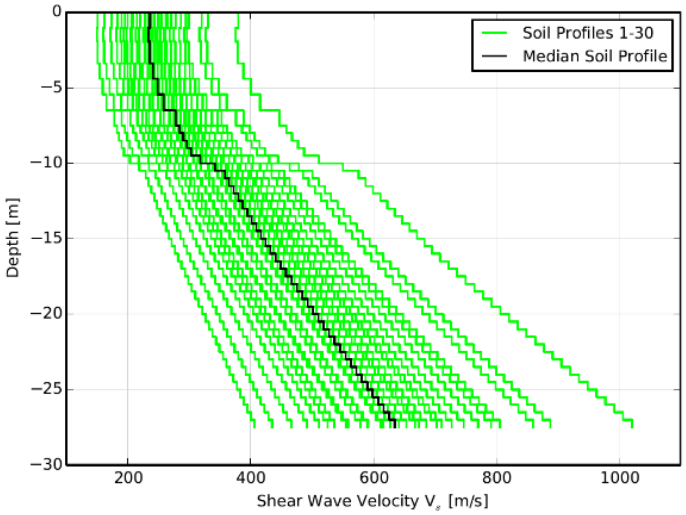

Figure 3. Generated 30 Strain-Compatible Soil Profiles for soil-structure interaction analysis.

MATERIAL PROPERTIES OF THE REACTOR BUILDING STRUCTURE

At Gösgen NPP a comprehensive Concrete Aging Program (CAP) is maintained which documents the concrete strength development for different buildings and building sections over time. As part of the CAP sufficient sample testing results are available from the plant construction period, the basic inspection (after 20 years of service), and the main inspection (after 30 years of service). The increase in concrete strength as described by the strength increase factor is determined to be 1.61 for the RB. The corresponding median Young's Modulus for reinforced concrete is calculated. In accordance with the EPRI (2013) guidance a median damping for reinforced concrete of 7 % of the critical damping is used. A damping of 4 % for structural steel, NSSS, and steel piping is applied.

The randomized parameters accounting for variability in structural properties were sampled to generate 30 scaling factors. The scaling factors which are computed using the LHS simulation method are applied to the median material properties to simulate the structural response due to variability in Modulus of Elasticity and damping of the reinforced concrete structure of the RB. A CoV of 0.35 (target 0.35) is used for the Modulus of Elasticity and 0.37 (target 0.35) for the damping. These assumptions yield scaling factors within the range of values between 0.33 and 2.02 for the elastic modulus and 0.41 and 2.30 for the damping. A negative correlation coefficient of -0.43 between modulus of elasticity and structural damping is considered. The restricted pairing sampling approach ensures physically reasonable randomized models.

3D FINITE-ELEMENT MODEL OF THE REACTOR BUILDING STRUCTURE

The data presented in this paper are based on a preliminary model of the reactor building. The detailed 3D finite-element model of the reactor building is characterized by the following details, (see Fig. 4): a) approx. 63 000 nodes; b) approx. 73 000 elements; c) approx. 380 000 degrees of freedom; d) total mass of approx. 160 000 t. The concrete shear walls and slabs of the structure are modelled with 3D thick-shell elements with three translational and three rotational degrees of freedom per node. The element formulation includes the out-of-plane shear stiffness. The steel containment, the cylindrical part of the reinforced concrete reactor building and its dome are modelled with 3D thin-shell elements with three translational and two rotational degrees of freedom per node. The out-of-plane translational degree of freedom is also included; however, transverse shear stiffness and the drilling rotational stiffness of the members are neglected. Structural columns and girder members are represented by beam elements with three translational and three rotational degrees of freedom per node. Material properties of concrete (stiffness and strength) include age hardening effects and are derived from core samples taken from the existing structure, see Rangelow et al. (2017).

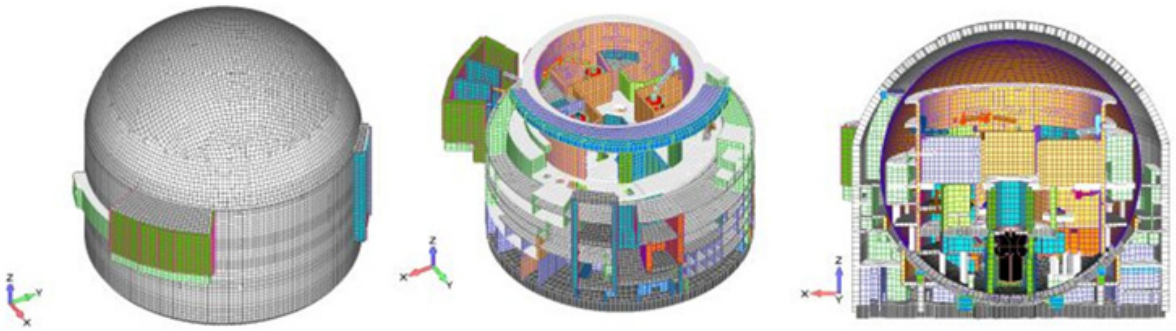

Figure 4. 3D Finite-Element Model of the Reactor Building Structure.

3D FINITE-ELEMENT MODEL OF THE NUCLEAR STEAM SUPPLY SYSTEM (NSSS)

The NSSS finite-element model (see Fig. 5) consists of the primary and secondary loops including the reactor pressure vessel, steam generators, reactor coolant pumps and lines, pressurizer, as well as main steam, and feedwater lines within the containment. The FE model is developed with ANSYS.

The primary coolant system components are modeled by a combination of elastic and rigid beam elements. Component suspensions (cross-beams and hangers) are represented by elastic beam elements. Lower and upper seismic supports are modeled with spring elements. Component masses (incl. content e.g. water filling, etc.) are lumped at selected model nodes. Pipes are represented by elastic beam elements. Elbow elements are modeled with stiffness matrix elements, see Rangelow et al. (2017).

COUPLED 3D FINITE-ELEMENT MODEL OF THE REACTOR BUILDING AND NSSS

For the SSI analysis the ANSYS model of the NSSS is ported to SASSI. The NSSS model and the RB structure are coupled at 189 nodes by rigid beam elements. Several modifications (e.g. unit conversion, consideration of local coordinate systems) are applied to ensure compatibility of the ANSYS NSSS model with the element library and specific features of SASSI. For verification and validation of the correct coupling of the NSSS model with the building model, the same ground motion time history is processed with two different analysis methods and software packages (frequency domain analysis in SASSI vs. modal time history analysis in ANSYS). In both cases flexibility is limited to the NSSS, whereas the building structure is rigid (see Fig. 6/left). In addition to verifying the primary circuit integration into the building model, simultaneously a cross-check of the software packages is accomplished, see Fig. 6/right.

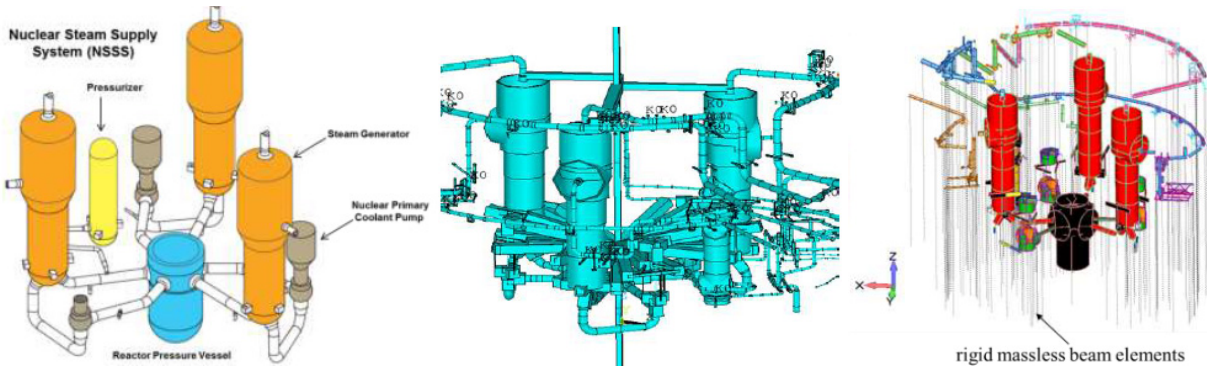

Figure 5. 3D Finite-Element Model of the Nuclear Steam Supply System.

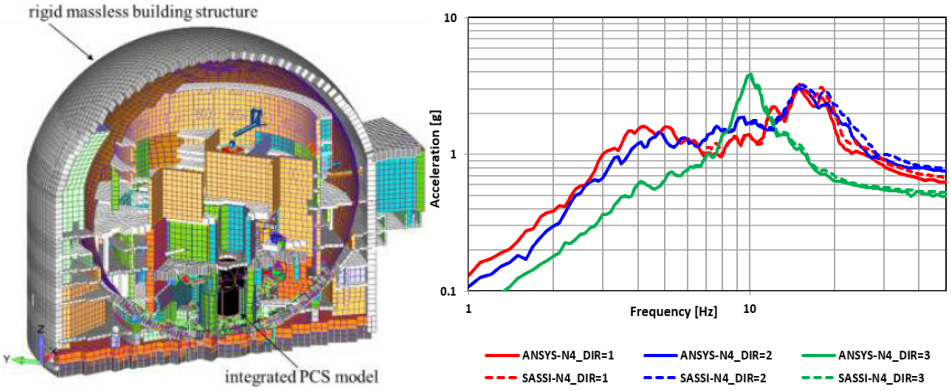

Figure 6. Left: NSSS model coupled with a massless and rigid structure model (SASSI);
Right: Verification of the SASSI Model: Comparison of ISRS: (ANSYS vs. SASSI)

CONSIDERATION OF GROUND MOTION INCOHERENCY

In general, the ground motion at different locations between subsurface medium and foundation differs in any time instance within a seismic event. This difference is commonly recognized as the incoherency in ground motion. The effect of incoherent ground motions is considered in this analysis to more realistically represent the high frequency response of the structure. Thereby, the Abrahamson soil plane-wave coherency model (EPRI, 2006) is utilized retaining a total of 10 coherency modes for analysis.

SOIL-STRUCTURE INTERACTION ANALYSIS APPROACH

Uncertainties and randomness in the seismic structural response analysis are accounted for by performing probabilistic SSI analyses of the coupled RB-NSSS model with parameter variability for ground motions, soil, and structural properties. The probabilistic SSI analyses are performed using SC-SASSI (2018), which operates in the frequency domain and outputs the seismic responses in the time domain.

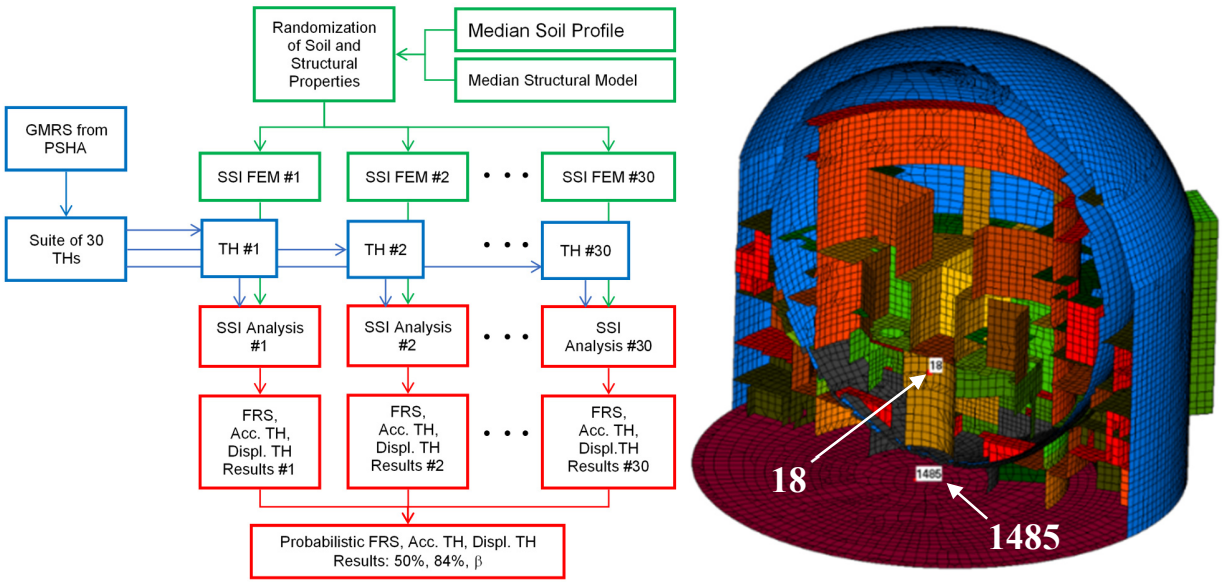

Figure 7. Left: Employed Probabilistic SSI Analysis Approach;
Right: Location of the Structural Model Nodes 18 and 1485 (Center of Basemat).

As shown in Fig. 7/left, the 30 SSI analysis models are generated by pairing the 30 soil profiles with 30 the structural models and the 30 sets of time histories. Each parameter is randomly sampled independently of any other parameter, except for the complementary correlation between stiffness and damping of both soil and structure. The 30 SSI analyses are performed for an embedded reactor building model with 7323 interaction nodes using the Extended Modified Subtraction Method (EMSM) modeling technique. The Direct Method (DM) analysis model which is used to validate the EMSM approach has a total number of 16958 interaction nodes. Each of the 30 SSI analyses is performed for a set of 110 discrete frequency values.

RESULTS OF THE PROBABILISTIC SOIL-STRUCTURE INTERACTION ANALYSIS

Fig. 7/right indicates the location of the two key structural nodes whose response is examined exemplarily in this paper. Fig. 8/top & bottom show the incoherent transfer functions in horizontal (X) direction for all 30 SSI-Models between the control point at foundation level (-9 m) and the nodes 1485 and 18. The 30 SSI models are generated by propagating the variability of the soil and structure parameters described above. This figure indicates significant variability of both fundamental frequencies and amplification amplitudes of the 30 SSI systems. As expected, the amplification of node 18 is larger because of its higher elevation in the building. There are two main locations with transfer function peaks: the first peak between 3 and 4 Hz, and the second between 10 and 11 Hz. Looking at the FIM spectra an unfavorable resonance situation is revealed: the two peaks of the seismic excitation are in the same frequency ranges, namely at 4 and approx. 11 Hz. A closer look at the three largest peaks of the transfer functions of node 18 at approx. 4 Hz (largest seismic demand) explains their existence, namely unfavorable (conservative) pairing of low damping values of both soil and structure. As is known, damping controls the peak response. For example, the run with the largest peak at approx. 3.7 Hz has scaling factors $0.50\times D_{soil}$ and $0.89\times D_{RB}$ (RB = reactor building structure). Since the generated damping is low, the transfer function peaks are expected to affect the variability of the in-structure-response spectra (ISRS) in the resonant frequency range significantly.

Fig. 9/top confirms this expectation. The variability of the calculated probabilistic ISRS for node 18 is large. It is noted that the ISRS contain not only the epistemic uncertainty represented by the transfer functions (i.e. model parameter) but also the randomness of the ground motion (aleatory uncertainty). Both epistemic and aleatoric uncertainty contribute to the total variability observed in the ISRS. The aleatory variability is governed by the variability of intensity measures other than the ground response spectra, notably duration, AI and CAV (recall section “Ground motion definition”). The effect of the aleatory variability is isolated by fixing the FE model properties (median) and performing additional 30 SSI analyses with the 30 THs. The transfer function of the “median” model (peak at 3 Hz) is shown in Fig. 8/bottom (black curve). Fig. 9/middle indicates a small aleatory variability due to the ground motion. It is noted that the “median” model is not in a resonance condition with the FIM. Spectral values of both figures (Fig. 9/top & middle) are normalized by the peak of the 50 %-fractile in Fig. 9/top.

By using the two sets of probabilistic results shown in Fig. 9, the model parameter variability (β_U) can be easily evaluated by subtracting (in SRSS sense) the randomness (β_R) based on Fig. 9/middle from the composite variability (β_C) based on Fig. 9/top. The result of this separation is shown in Fig. 9/bottom. It shows that the low frequency range below approx. 1.5 Hz is dominated in this particular case by the ground motion randomness (β_R) and the intermediate and high frequency range by the variability of the model parameters (β_U), incl. the zero-period-acceleration (ZPA) value. It is noted that the ZPA value in a response spectrum corresponds to the maximum response of the primary system (building structure), whereas the maximum response of a secondary system attached to the primary system (e.g. component idealized as a single degree of freedom system) is a function of its fundamental frequency. In analogy, the frequency dependent variability derived from the ISRS and shown in Fig. 9/bottom should be interpreted accordingly. The intermediate frequency range exhibits a narrow peak at approx. 3.7 Hz (recall the discussion of Fig. 8/bottom) with a logarithmic standard deviation value (β_U) of almost 1.0. This peak corresponds to a resonance state, where the fundamental frequency of the SSI system (transfer function peak) coincides with the peak of the seismic excitation (Fig. 2). The three SSI models (out of 30) in

resonance state (see Fig. 8/bottom) with unfavorably low LHS scaling factors for damping are primarily responsible for the β_C peak. From a physical point of view, the seismic capacity of a component in resonance state with an estimated large variability in the linear dynamic response will heavily depend on its ductile energy absorption mechanism.

In addition to the frequency-dependent β_C, β_U, and β_R values, Fig. 9/bottom shows the frequency-independent, generic β–values from EPRI (2013), where the composite variability is stated to range $0.3 < \beta_C < 0.6$. The frequency-dependent β–values based on probabilistic ISRS are either within or below that range, except a narrow range at 3.7 Hz. Even in that range a direct propagation of the large variability to the failure-governing stresses is unlikely (inelastic energy absorption). Considering that in a median-based fragility analysis large variability implies a low HCLPF, it can be stated that the β–values based on probabilistic ISRS are compatible with generic β–values from EPRI (2013), with a slight conservative bias.

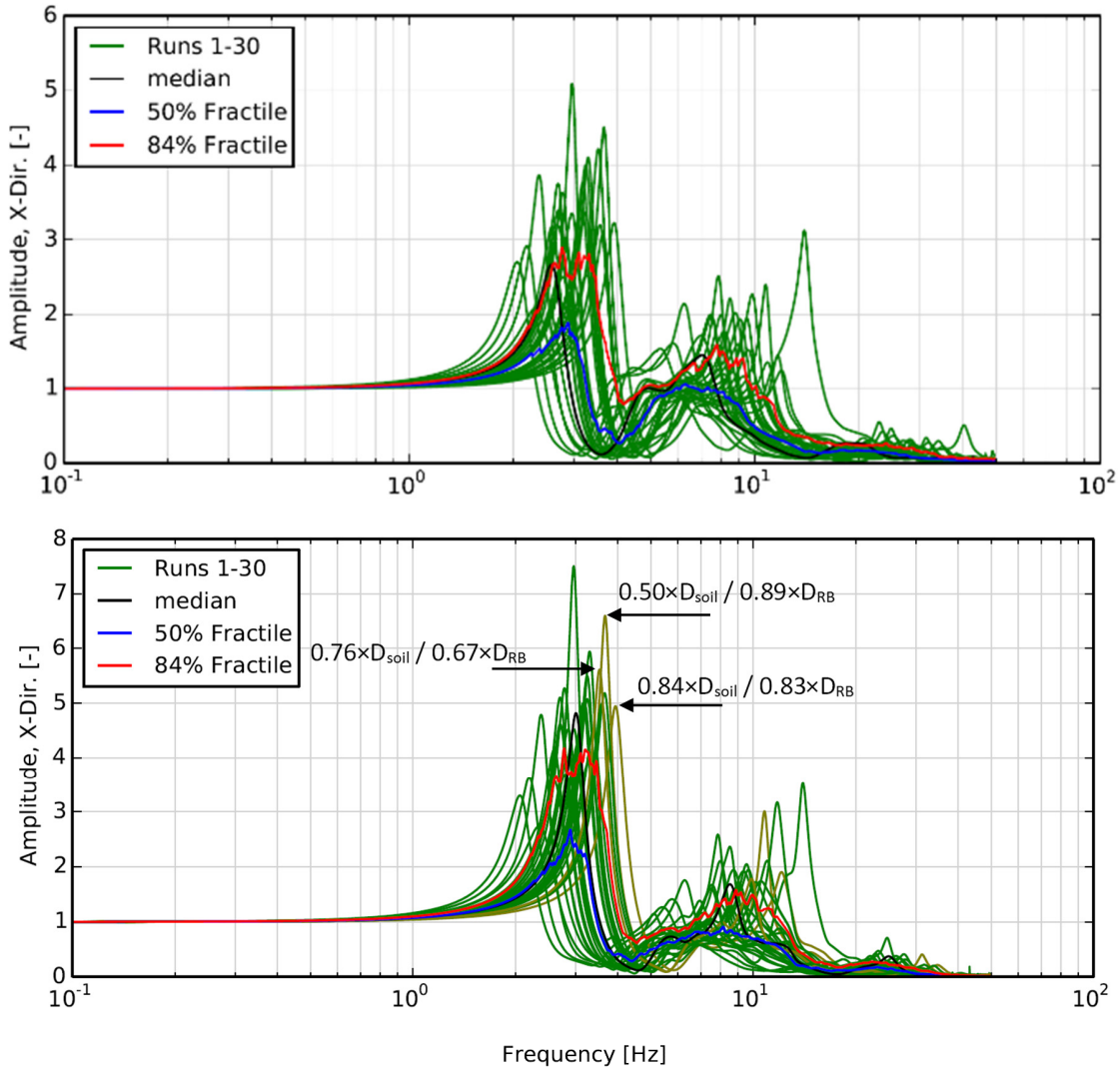

Figure 8. Transfer Functions for all 30 SSI-Models in Horizontal (X) Direction between Control Point at Foundation Level and Structural Nodes Top: Node 1485 (Center of Basemat); Bottom: Node 18.

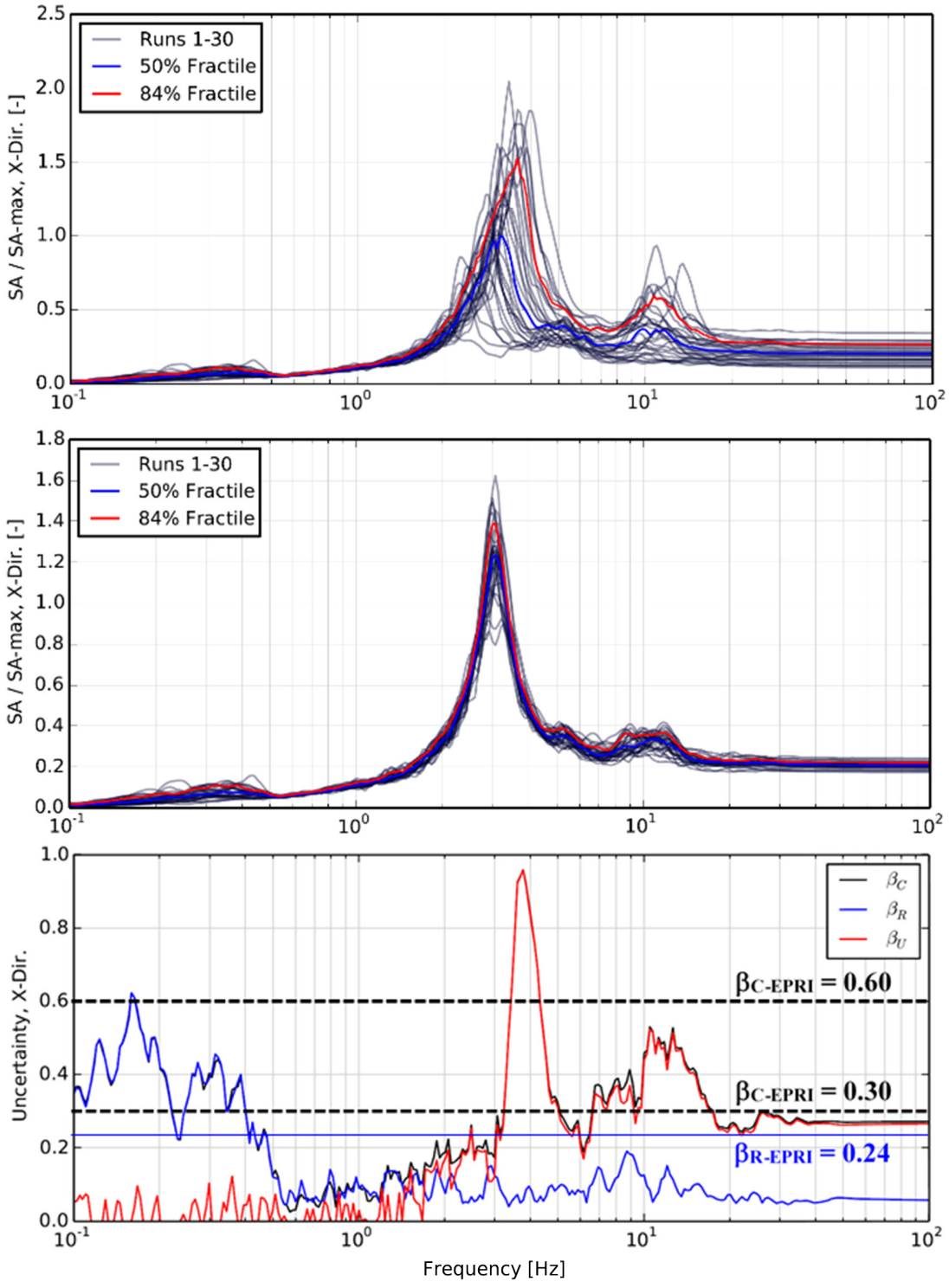

Figure 9. Probabilistic ISRS in Horizontal (X) Direction for Node 18, D = 5 %
Top: Results for all 30 SSI-Models; Middle: Results for the Best-Estimate (Median) SSI-Model.
Bottom: Separation of the Composite Variability (β_C) into Randomness (β_R) and Uncertainty (β_U).

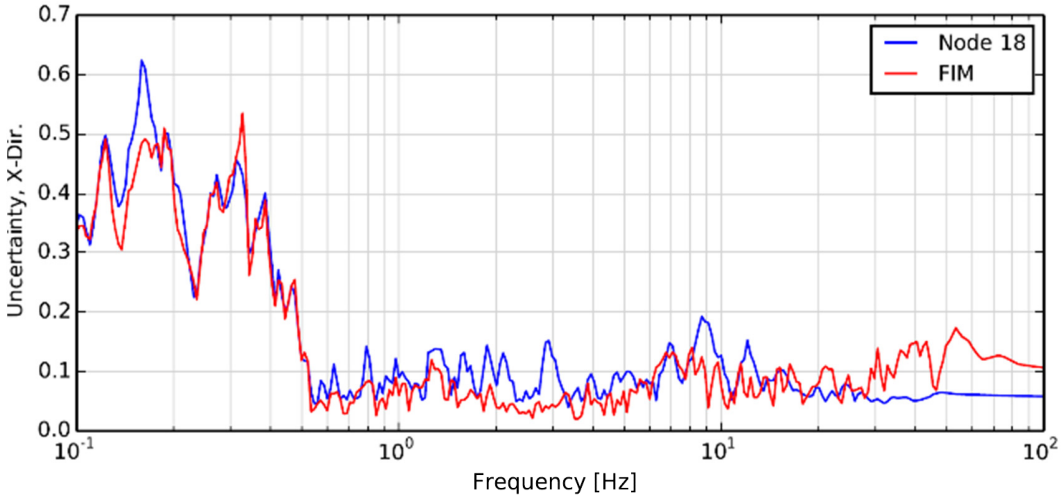

Figure 10. Node 18 in Horizontal (X) Direction: Comparison of the Randomness (β_R) estimated from the 30 FIM Spectra (Fig. 2) vs. the Randomness estimated with the Median SSI-Model (Fig. 12; bottom).

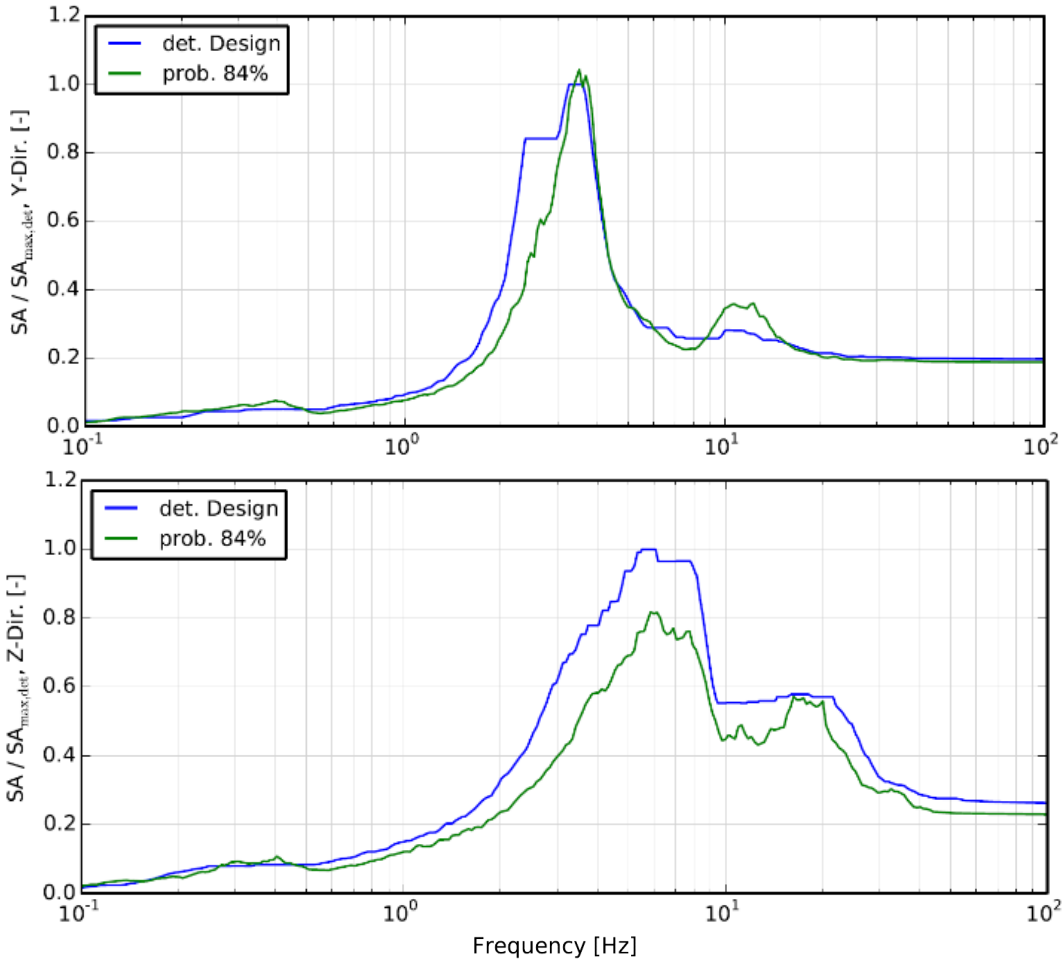

Figure 11. Comparison of the 84 % NEP Probabilistic vs. Deterministic Spectra at Node 18, D = 5 %; Top: in Horizontal (Y) Direction; Bottom: in Vertical (Z) Direction.

Fig. 10 confirms the low contribution of the randomness (β_R) to the composite variability, with values lower than the recommended value of $\beta_R = 0.24$ by EPRI, except for frequencies below 0.4 Hz. It also shows that β_R values estimated from the 30 UHS-compatible FIM response spectra (Fig. 2) fit quite well to those estimated with the median SSI-model (Fig. 9/middle). The small discrepancy could be attributed to the incoherent transfer function used with the median SSI-model as well as numerical approximations.

Fig. 11 presents a comparison of ISRS between the deterministic Design Response Spectra (DRS) and the probabilistic 84% Non-Exceedance Probability (NEP) responses of node 18 for both horizontal and vertical directions. Ordinates of both figures are normalized by the deterministic spectral peak. It shows that the probabilistic spectra for 84% NEP are in good agreement with the deterministic spectra.

CONCLUSION

In this paper the coupled 3D Reactor-Building-Nuclear-Steam-Supply-System finite-element model, the methodology utilized in probabilistic SSI analysis, preliminary probabilistic results (e.g. ISRS and their frequency dependent variability), insights gained from the probabilistic ISRS, and their applicability for the fragility analysis are presented. The associated deterministic analysis results were presented by Nykyforchyn et. al. (2018).

Probabilistic ISRS and frequency dependent β_C, β_U, and β_R values are evaluated in this study. The composite variability (β_C) is dominated by random ground motion variability (β_R) in the low frequency range (below 2 Hz) and by uncertainty associated with model parameters (β_U) in the intermediate and high frequency range. In the intermediate frequency range the variability exhibits a narrow peak at approx. 3.7 Hz with a β_U of almost 1.0. This peak corresponds to a resonance state, where the fundamental frequency of few SSI systems out of 30 in this study coincides with the peak of the seismic excitation. From a physical point of view, the seismic capacity of a component in such resonance state with an estimated large variability in the dynamic response will heavily depend on its ductile energy absorption mechanism. Keeping this in mind, the frequency-dependent β–values based on probabilistic ISRS are compatible with the generic β–values ($0.3 < \beta_C < 0.6$) in EPRI (2013), with a slight conservative bias.

Finally, the probabilistic spectra for 84% NEP in this study are in good agreement with the deterministic spectra.

REFERENCES

Electric Power Research Institute, EPRI. (2006). Program on Technology Innovation: Spatial Coherency Models for Soil-Structure Interaction. Report Nr. 1014101, Palo Alto, USA.

Electric Power Research Institute EPRI. (2013). SPID for the Resolution of Fukushima Near-Term Task Force Recommendation 2.1: Seismic, Report No. 1025287, Palo Alto, California, USA.

Nykyforchyn A., Stäuble, S., Rangelow, P., Richter, T., Nincic, V., Pellissetti, M. (2018). Comprehensive Deterministic Seismic Analysis of a Coupled 3D Model of Reactor Building and NSSS, Technological Innovations in Nuclear Civil Engineering, TINCE 2018, Paris-Saclay, France.

Rangelow, P., Schneider, O., Hilpert, R., Schramm, K., Pellissetti, M., Nykyforchyn, A., Stäuble, S. (2017). "Response of a Nuclear Power Plant Building under Incoherent Seismic Ground Motion Excitation", 16th World Conference on Earthquake, Chile.

SC Solutions. (2018). SC-SASSI, Version 2.3.2. Sunnyvale, California, USA.

Stäuble-Akcay, S., Nykyforchyn, A., Klügel, J.U. (2018). Seismic safety reassessment of NPP Gösgen after completion of site-specific probabilistic seismic hazard analysis. 16th ECEE, Greece.

US Nuclear Regulatory Commission, NRC. (2014). Standard Review Plan - 3.7.1 Seismic Design Parameters NUREG-0800 Revision 4, Washington DC, USA.